

SN 2010jl IN UGC 5189: YET ANOTHER LUMINOUS TYPE II_n SUPERNOVA IN A METAL-POOR GALAXY

R. STOLL¹, J. L. PRIETO^{2,5}, K. Z. STANEK^{1,3}, R. W. POGGE^{1,3}, D. M. SZCZYGIEL¹, G. POJMAŃSKI⁴, J. ANTOGNINI¹, AND H. YAN³

¹ Department of Astronomy, The Ohio State University, 140 W 18th Ave, Columbus, OH 43210, USA; stoll@astronomy.ohio-state.edu

² Carnegie Observatories, 813 Santa Barbara Street, Pasadena, CA 91101, USA

³ Center for Cosmology and AstroParticle Physics, The Ohio State University, 191 West Woodruff Avenue, Columbus OH 43210, USA

⁴ Warsaw University Astronomical Observatory, Al. Ujazdowskie 4, 00-478 Warsaw, Poland

Received 2010 December 15; accepted 2011 January 18; published 2011 March 1

ABSTRACT

We present All-Sky Automated Survey data starting 25 days before the discovery of the recent type II_n SN 2010jl, and we compare its light curve to other luminous II_n supernovae (SNe), showing that it is a luminous ($M_I \approx -20.5$) event. Its host galaxy, UGC 5189, has a low gas-phase oxygen abundance ($12 + \log(\text{O}/\text{H}) = 8.2 \pm 0.1$), which reinforces the emerging trend that overluminous core-collapse supernovae (CCSNe) are found in the low-metallicity tail of the galaxy distribution, similar to the known trend for the hosts of long GRBs. We compile oxygen abundances from the literature and from our own observations of UGC 5189, and we present an unpublished spectrum of the luminous type Ic SN 2010gx that we use to estimate its host metallicity. We discuss these in the context of host metallicity trends for different classes of core-collapse objects. The earliest generations of stars are known to be enhanced in [O/Fe] relative to the solar mixture; it is therefore likely that the stellar progenitors of these overluminous SNe are even more iron-poor than they are oxygen-poor. A number of mechanisms and massive star progenitor systems have been proposed to explain the most luminous CCSNe. Any successful theory that tries to explain these very luminous events will need to include the emerging trend that points toward low metallicity for the massive progenitor stars. This trend for very luminous SNe to strongly prefer low-metallicity galaxies should be taken into account when considering various aspects of the evolution of the metal-poor early universe, such as enrichment and reionization.

Key words: galaxies: abundances – stars: massive – supernovae: general – supernovae: individual (SN 2010jl, SN 2010gx)

Online-only material: color figures

1. INTRODUCTION

The bright SN 2010jl, discovered on UTC 2010 November 3.5 (Newton & Puckett 2010) was classified as a type II_n supernova (SN; Benetti et al. 2010; Yamanaka et al. 2010). A possible luminous blue progenitor has been identified in archival *Hubble Space Telescope* WFPC2 data (Smith et al. 2010b). If this detection is of a massive compact cluster, the turnoff mass is constrained to be $>30 M_{\odot}$. If it is a single star, it is either a massive η Carinae-like star or something fainter that has been caught in a luminous blue variable (LBV)-like eruption phase, possibly a precursor explosion. Spectropolarimetric observations indicate possible asymmetry in the explosion geometry and limit the amount of dust in the progenitor environment (Patat et al. 2010).

Prieto & Stanek (2010) point out that the SN’s host galaxy, UGC 5189, has been shown to be metal-poor based on a spectrum obtained by the Sloan Digital Sky Survey (SDSS) a few arcseconds away from the site of the SN. It is included in the Tremonti et al. (2004) DR4 catalog of galaxy metallicities, which estimates $12 + \log(\text{O}/\text{H}) = 8.15 \pm 0.1$ dex based on strong recombination and forbidden emission lines in the spectrum. Pilyugin & Thuan (2007) estimate $12 + \log(\text{O}/\text{H}) = 8.3$ dex from the same spectrum based on the “direct” photoionization-based abundance method using an estimate of the electron temperature (T_e) from the [O III] λ 4363 Å auroral line.

Throughout this paper, as above, we will adopt O/H as a proxy for the “metallicity” of the host galaxy, because only gas-

phase oxygen abundance estimates are available. In Section 4, we will discuss how this relates to total metal abundance and iron abundances.

There is mounting evidence showing that the majority of the most optically luminous SNe explode in low-luminosity, star-forming galaxies, which are likely to be metal-poor environments. Circumstantial evidence comes from the fact that most of these objects have been discovered in new rolling searches that are not targeted to bright galaxies, even though they were bright enough to be discovered in galaxy-targeted searches (the only exception is the recently discovered SN 2010jl). Some of the rolling searches that are discovering the most energetic SNe include the Texas Supernova Search (TSS; Quimby 2006), the Catalina Real-Time Transient Survey (Drake et al. 2009), the Palomar Transient Factory (PTF; Rau et al. 2009), and the Panoramic Survey Telescope & Rapid Response System (Pan-STARRS). Neill et al. (2011) find that luminous SNe occur predominantly in the faintest, bluest galaxies. Li et al. (2010) find that SNe II_n may preferentially occur in smaller, less-luminous, later-type galaxies than SNe II-P. The mass–metallicity relationship implies that such small, faint galaxies should tend to be low metallicity (Tremonti et al. 2004).

Kozłowski et al. (2010) presented the first host galaxy luminosity versus oxygen abundance diagram with a small sample of three energetic type II_n and type Ic core-collapse supernovae (CCSNe) compiled from published work in the literature (two objects) and new data for SN 2007va. These initial results suggest that the host galaxy environments of the most energetic CCSNe are on average metal-poor (metallicities $\sim 0.2\text{--}0.5 Z_{\odot}$) compared to the bulk of star-forming galaxies in SDSS and are similar in metallicity to the hosts of local GRBs

⁵ Hubble and Carnegie-Princeton Fellow.

Table 1
Optical Photometry of SN 2010jl

HJD −2450000	<i>U</i> (mag)	σ	<i>B</i> (mag)	σ	<i>V</i> (mag)	σ	<i>R</i> (mag)	σ	<i>I</i> (mag)	σ	Telescope
5479.14	13.79	0.10	ASAS
5484.13	13.73	0.10	13.28	0.10	ASAS
5488.12	13.67	0.10	13.09	0.10	ASAS
5493.14	13.73	0.10	ASAS
5494.12	13.00	0.10	ASAS
5504.10	13.78	0.10	13.10	0.10	ASAS
5509.10	13.86	0.10	ASAS
5509.13	13.18	0.10	ASAS
5515.75	13.83	0.05	14.24	0.05	13.46	0.05	13.85	0.05	13.19	0.05	Swope
5516.75	13.83	0.05	14.26	0.05	13.45	0.05	13.87	0.05	Swope
5517.13	13.28	0.10	ASAS
5517.75	13.86	0.05	14.26	0.05	13.87	0.05	13.20	0.05	Swope

(Stanek et al. 2006). It has now been well established that long GRBs are accompanied by broad-line type Ic SNe (e.g., Stanek et al. 2003), firmly connecting these very energetic explosions to the deaths of massive stars. In contrast, luminous type II_n SNe are not shown to be connected with local GRBs (although see Germany et al. 2000; Rigon et al. 2003). The sample of luminous SNe with measured abundances is small and incomplete because only some of the brightest host galaxies have been targeted, which hinders the interpretation and comparison of the results.

In this paper, we expand this sample with metallicities of the hosts of SN 2010gx and SN 2010jl and put all metallicity measurements on a common scale to confirm the emerging trend that these optically luminous core-collapse events appear to occur in low-metallicity or low-luminosity hosts.

2. OBSERVATIONS

2.1. Photometry

Photometric data were obtained with the 10 cm All-Sky Automated Survey (ASAS) North telescope in Hawaii (Pojmanski 2002; Pigulski et al. 2009). These data were processed with the reduction pipeline described in detail in Pojmanski (1998, 2002). The *V* magnitudes are tied to the Johnson *V* scale using Tycho (Høg et al. 2000) and Landolt (Landolt 1983) standard stars. The *I* magnitudes were calibrated using transformed SDSS DR7 (Abazajian et al. 2009) magnitudes of standards in the field. The magnitudes were measured using aperture photometry with a 2 pixel (30 arcsec) aperture radius. We subtract the contribution from the host galaxy measuring the median magnitude of the host in the same aperture using all archival ASAS images before the SN, which give $V_{\text{host}} = 14.97$ mag and $I_{\text{host}} = 14.28$ mag.

We obtained *UBVRI* images of SN 2010jl with the SITE-3 CCD camera mounted on the Swope 1 m telescope at Las Campanas Observatory on three consecutive nights from UT 2010 November 15–17. The images were reduced with standard tasks in the IRAF⁶ ccdproc package. The data were flat-fielded using domeflats obtained for *BVRI* images and twilight skyflats for *U*-band images. We applied a linearity correction using the prescription and coefficients from Hamuy et al. (2006). The photometry of the SN was obtained using aperture photometry and a 2'' radius aperture with the phot task in IRAF. The

magnitudes were calibrated using field stars with SDSS DR7 *ugriz* photometry, converted to standard *UBVRI* magnitudes through standard equations on the SDSS Web site. We subtracted the contribution from the host galaxy fluxes measuring the magnitudes in the same aperture using the pre-explosion SDSS images. In Table 1, we gather all optical photometry presented in this paper.

2.2. Spectroscopy

Spectra were obtained on 2010 November 5 and November 11 with the Ohio State Multi-Object Spectrograph (OSMOS; Martini et al. 2011; Stoll et al. 2010) on the 2.4 m Hiltner telescope. The OSMOS slit was oriented N/S. Although the instrument supports a 20 arcmin long slit, we observed the target with the CCD readout in a subframe that limited the effective slit length to 5 arcmin to reduce the readout time. A schematic of the slit coverage on the field is shown in Figure 1. The 1.2 arcsec slits we used in the OSMOS observations are shown with black rectangles. The irregular galaxy has four archival SDSS spectra; the locations of the SDSS fiber apertures are shown with red circles.

We processed the raw CCD data using standard techniques in IRAF, including cosmic ray rejection using L.A.Cosmic (van Dokkum 2001). Each source was extracted individually with apall, extracting a sky spectrum simultaneously. The range of extraction apertures was 14–24 pixels, corresponding to 3.8–6.6 arcsec, or 0.8–1.4 kpc at the distance of UGC 5189. With the 1.2 arcsec slit used in our observations, the OSMOS VPH grism provides $R \sim 1600$ at 5000 Å. The red slit position we used provides a wavelength coverage of 3960–6880 Å. Wavelength calibration was done with Ar arc lamp observations, and a spectrophotometric standard from Oke (1990) was observed each night, with which we performed relative flux calibrations.

The top panel of Figure 2 shows a spectrum of SN 2010jl obtained on November 5. Taking advantage of the N/S slit, we extract host galaxy spectra centered ~ 7 arcsec on either side of the SN, corresponding to ~ 1.5 kpc at the distance of UGC 5189. In Section 3.2, we use strong-line abundance diagnostics on these host galaxy spectra to estimate the gas-phase oxygen abundances of the progenitor environment.

We also present in this paper a previously unpublished spectrum of the luminous ($M_B \approx -21.2$) type Ic SN 2010gx (Pastorello et al. 2010) obtained with the WFCCD imager and spectrograph on the du Pont 2.5 m telescope at Las Campanas Observatory using a long slit mask (slit width 1'') and the 300 l mm^{−1} grism. We obtained 1200 s spectra on

⁶ IRAF is distributed by the National Optical Astronomy Observatory, which is operated by the Association of Universities for Research in Astronomy (AURA) under cooperative agreement with the National Science Foundation.

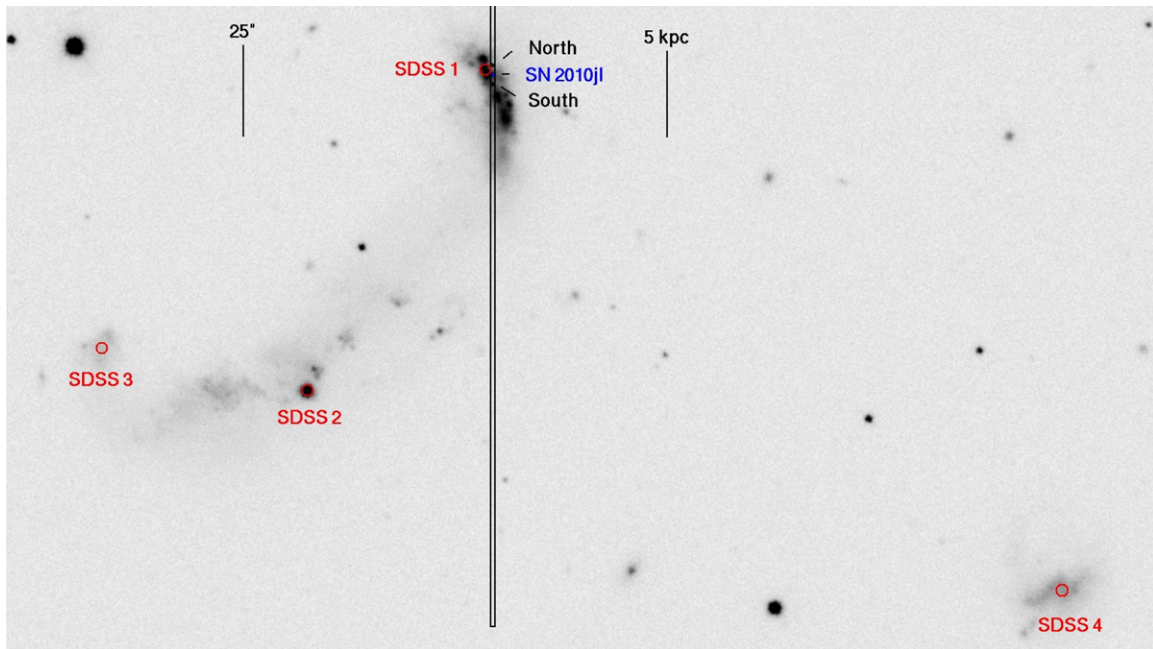


Figure 1. Schematic of the host galaxy of SN 2010jl. North is up and east is to the left. The OSMOS slit position is marked with a black rectangle 1.2 arcsec wide. The slit was centered on the supernova. The fiber positions of archival SDSS spectra of the galaxy are marked with the red circles, which have a diameter of 3 arcsec. The background is constructed from SDSS g imaging. The small blue galaxy in the southwest corner of the image has a similar spectrum and is at the same redshift ($z = 0.0107$). It is almost certainly part of the interacting system. The position of SN 2010jl is marked, as well as the emission regions to the north and south for which we extract OSMOS spectra.

(A color version of this figure is available in the online journal.)

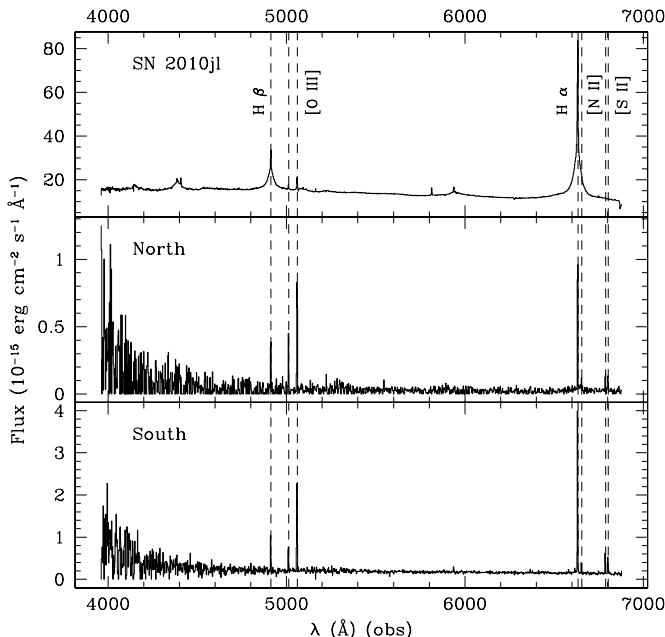


Figure 2. OSMOS spectra of SN2010jl and the emission line regions ~ 7 arcsec (~ 1.4 kpc) to the north and south. Negative flux values from noise have been truncated to zero. Dashed lines show the wavelengths of $H\beta$ $\lambda 4861$, $[O\text{ III}]\lambda 4959, 5007$, $H\alpha$ $\lambda 6563$, $[N\text{ II}]\lambda 6584$, and $[S\text{ II}]\lambda 6717, 6731$ at $z = 0.0107$.

three consecutive nights (UT 2010 March 22–24), or 4 ± 2 days (rest frame) prior to the B -band peak. The WFCCD data were reduced using standard tools in IRAF. We derived the wavelength solutions with He–Ne–Ar arcclamps obtained after each spectrum and did independent relative flux calibration using spectrophotometric standards observed each night. The

final spectrum in Figure 3 is a combination of the three individual exposures, obtained in order to increase the signal-to-noise ratio (S/N). The spectrum covers the wavelength range 3700–9200 Å and has an FWHM resolution of ~ 7 Å. Assuming a Galactic reddening law with $R_V = 3.1$, the total V -band extinction was estimated to be $A_V = 0.27$ mag using the ratio of $H\alpha$ to $H\beta$ fluxes and correcting to the theoretical case-B recombination value of 2.85. The spectrum was corrected for this reddening before calculating line ratios. The continuum was subtracted locally to each emission line before measuring the flux; the effect of the SN contamination on the metallicity determination should be small. We estimate the oxygen abundance to be $12 + \log(O/H) = 8.36$ using the diagnostic of Kobulnicky & Kewley (2004), which uses $R_{23} = ([O\text{ II}]\lambda 3727 + [O\text{ III}]\lambda 4959, 5007) / H\beta$ and $O_{32} = ([O\text{ III}]\lambda 5007 + [O\text{ III}]\lambda 4959) / [O\text{ II}]\lambda 3727$. These are highly sensitive to reddening, so the correction is crucial. (In subsequent discussion, we convert this metallicity to the scale of Pettini & Pagel 2004 for uniformity.)

3. RESULTS AND ANALYSIS

3.1. SN 2010jl Light Curve

The ASAS light curves of SN 2010jl include several pre-peak observations beginning 25 days before discovery. We plot them in Figure 4 along with the V - and I -band Swope data. For comparison, we plot R -band light curves from the literature of the ultraluminous SN 2006gy (Smith et al. 2007) and SN 2006tf (Smith et al. 2008), and the luminous type II n SN 1998S (Fassia et al. 2000). UGC 5189 was behind the Sun and unobservable prior to the first ASAS observations. The color of the SN changed from $V - I \approx 0.4$ mag at the epoch of ASAS discovery to $V - I \approx 0.7$ mag at the latest epochs. The $UBVRI$ photometry from Swope is consistent with a ~ 7000 K blackbody, as Smith et al. (2010b) conclude from

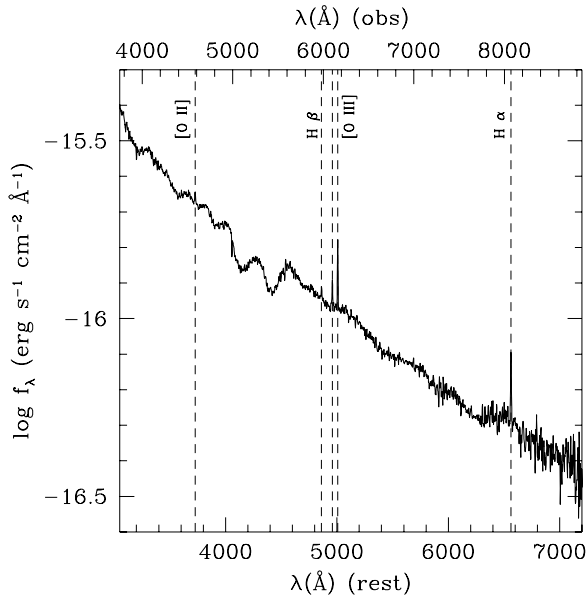


Figure 3. Spectrum of the luminous SN 2010gx obtained with the du Pont 2.5 m telescope at the Las Campanas Observatory in 2010 March, before the supernova reached maximum light. The spectrum has a blue continuum with broad ($\sim 10,000$ km s^{-1}) absorption features likely associated with ionized oxygen, nitrogen, and carbon. Although the nature of these events is still under debate, they share characteristics that are similar to the spectra of SN Ib/c (Quimby et al. 2009; Pastorello et al. 2010). The dashed lines mark the wavelengths of narrow emission lines of [O II] λ 3727, H β λ 4861, [O III] λ 4959, 5007, and H α λ 6563 detected from the star-forming host galaxy. Using these lines, we can estimate an oxygen abundance for the host of SN 2010gx of $12 + \log(O/H) = 8.36$, using the strong-line diagnostic of Kobulnicky & Kewley (2004). This corresponds to $\sim 0.3 Z_{\odot}$, similar to the metallicity of the LMC. In subsequent figures, we convert this value to the scale of the N2 diagnostic of Pettini & Pagel (2004), giving $12 + \log(O/H) = 8.16$.

a fit to the spectrum. The normal range for peak luminosities of type IIIn SNe is $-18.5 \lesssim M_R \lesssim -17$ (Kiewe et al. 2010). The pre-discovery ASAS data constrain the peak luminosity of SN 2010jl ($M_V \approx -19.9$, $M_I \approx -20.5$), placing it firmly in the class of luminous (peak $M_R < -20$) type IIIn SNe.

3.2. Metallicity Near SN 2010jl

We use the empirical O3N2 and N2 diagnostics of Pettini & Pagel (2004) and the theoretical and empirical N2 diagnostic of Denicoló et al. (2002) to determine the metallicity of the OSMOS-observed H II regions south and north of SN 2010jl. We choose these diagnostics based on the S/N and wavelength coverage of our observations. The N2 diagnostics of Pettini & Pagel (2004) and of Denicoló et al. (2002) depend solely on [N II] λ 6584/H α λ 6563. This ratio is very insensitive to reddening due to the proximity of the lines. The O3N2 diagnostic of Pettini & Pagel (2004) also depends on [O III] λ 5007/H β λ 4861, another closely spaced pair of lines. Although we do not correct these spectra for reddening, any reddening effect is very small compared to the scatter in each abundance diagnostic. For subsequent analysis in Section 3.4, we convert metallicities of other galaxies determined using other diagnostics to these scales to enable direct comparison, using the empirical conversions of Kewley & Ellison (2008).

For the galactic H II regions ~ 7 arcsec (~ 1.5 kpc) south and north of the SN site, using the Pettini & Pagel (2004) O3N2 diagnostic, we find $12 + \log(O/H) = 8.2 \pm 0.1$ dex. Using the N2 diagnostic, we find $12 + \log(O/H) = 8.2 \pm 0.1$ dex for the H II region north of the SN and 8.3 ± 0.1 dex for the one to

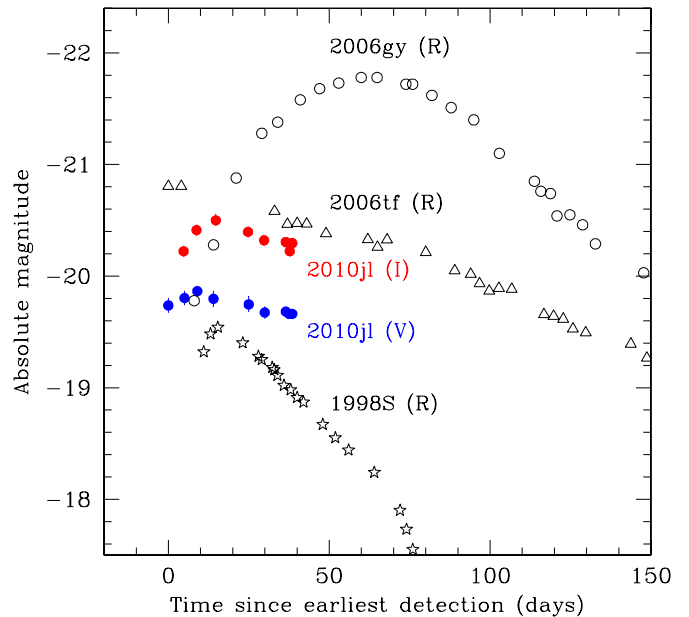


Figure 4. Absolute magnitude light curve of SN 2010jl, plotted for comparison with other type IIIn supernovae from the literature. The filled circles show the V - and I -band light curves of SN 2010jl from ASAS North and Swope. For all the other SNe we show the R -band light curves: the ultraluminous SN 2006gy (open circles; Smith et al. 2007) and 2006tf (open triangles; Smith et al. 2008), and the type IIIn 1998S (Fassia et al. 2000). The normal range of peak luminosities for type IIIn SNe is $-18.5 \lesssim M_R \lesssim -17$ (Kiewe et al. 2010). The horizontal axis is the time with respect to the earliest detection. In the case of SN 2010jl, the SN was discovered on 2010 November 3.5 (Newton & Puckett 2010), but the first detection from ASAS North is from 2010 October 9.6, 25 days earlier. (A color version of this figure is available in the online journal.)

the south. Using the Denicoló et al. (2002) diagnostic, we find $12 + \log(O/H) = 8.2 \pm 0.1$ dex and 8.4 ± 0.1 dex for the north and south regions, respectively.

Our estimates of the oxygen abundance are consistent with previously published estimates for UGC 5189 based on the SDSS spectrum from ~ 5 arcsec (~ 1 kpc) to the northeast of the SN site. Tremonti et al. (2004) report $12 + \log(O/H) = 8.15 \pm 0.1$ dex for this galaxy, based on strong recombination and forbidden emission lines. Pilyugin & Thuan (2007) report $12 + \log(O/H) = 8.3$ dex from the same spectrum based on direct electron temperature using the [O III] λ 4363 auroral line. For our analysis in Section 3.4 we convert the Tremonti et al. (2004) metallicities, but for lack of an established empirical conversion, we omit the Pilyugin & Thuan (2007) metallicities.

3.3. Metallicity Elsewhere in the Host Galaxy

There are two other SDSS spectra of the galaxy (see Figure 1), including a bright point source in the south, approximately 20 kpc from the location of the SN, marked in Figure 1 as SDSS 2. Pilyugin & Thuan (2007) report $12 + \log(O/H) = 8.3$ dex for this spectrum. The detection of He II λ 4686 Å indicates that the ionizing continuum is hard (e.g., Garnett et al. 1991), outside the regime where the Pettini & Pagel (2004) and Denicoló et al. (2002) diagnostics are valid. Brinchmann et al. (2008) include this spectrum in their SDSS-based study of nearby galaxies with Wolf-Rayet features. Tremonti et al. (2004) do not fit a metallicity to this spectrum despite the high S/N, presumably because of the peculiar line ratios.

The other SDSS spectrum is of the eastern-most clump of UGC 5189, approximately 30 projected kpc from the location of the SN (marked in Figure 1 as SDSS 3). Neither Tremonti et al.

(2004) nor Pilyugin & Thuan (2007) derive metallicities from this spectrum, which has lower S/N. We find $12 + \log(\text{O}/\text{H}) = 8.2 \pm 0.1$ dex with all three line ratio diagnostics using the SDSS spectrum.

Approximately 40 projected kpc from SN 2010jl is another blue galaxy at the same redshift (0.0106), which also has an SDSS spectrum, marked in Figure 1 as SDSS 4. The redshift of the spectrum from the SN site is 0.0107; these redshifts are consistent within the estimated 0.0001 redshift error for this lower S/N spectrum. From the shape and orientation of the wildly irregular UGC 5189, it seems very likely that this neighbor is a part of the interacting system. Using the SDSS spectrum, we find $12 + \log(\text{O}/\text{H}) = 8.2 \pm 0.1$ dex with both Pettini & Pagel (2004) diagnostics and 8.3 ± 0.1 dex with Denicoló et al. (2002).

UGC 5189 appears to be a high-mass, metal-poor outlier from the mass–metallicity relationship (e.g., Peeples et al. 2009). Such similar metallicity measurements from widely spaced locations and widely varying diagnostics provide reassurance that there are no significant metallicity variations in UGC 5189, and that the three metallicity measurements described in Section 3.2 from a kpc or more away from the SN site are likely to well describe the SN progenitor region. All evidence points toward a SN 2010jl metallicity of $\lesssim 0.3 Z_{\odot}$.

3.4. Host Metallicity Trends

The low metallicity of the host of SN 2010jl is another confirmation of the emerging trend of low-metallicity hosts of very luminous SNe (Kozłowski et al. 2010). In Figure 5, we show this trend for SN 2010jl (green squares) and other luminous SNe (blue pentagons; SN 2003ma, SN 2007bi, SN 2007va, and SN 2010gx). The oxygen abundance measurement for the host of SN 2010gx was obtained from our own spectroscopic observations, which we present here. The luminous SNe without detected hydrogen (SN 2010gx and SN 2007bi) are indicated with double pentagons. We plot three metallicity measurements for the host region of SN 2010jl with green squares: two from our OSMOS spectra of the regions ~ 1 kpc north and south of the SN and one from the SDSS spectrum ~ 1 kpc northeast of the SN; the value from strong-line fitting published by Tremonti et al. (2004). We cannot convert the Pilyugin & Thuan (2007) measurement of 8.3 to the scale of the Pettini & Pagel (2004) N2 diagnostic and so to maintain a strictly uniform abundance scale we do not plot it here. All four are consistent to within the errors, indicating that there is no strong metallicity variation in the area and that the strong-line diagnostics are well behaved and not in the poorly calibrated regime of very hard radiation fields. For comparison, we also plot contours showing the distribution of the measured SDSS galaxy metallicities from Tremonti et al. (2004). We also plot for comparison the medians and ranges of nebular abundances measured in the LMC and SMC with strong-line diagnostics from H II flux ratios reported by Russell & Dopita (1990) and absolute B magnitudes from Karachentsev (2005). We stress that the actual range in the LMC and SMC metallicities is likely lower than the range given by applying the Pettini & Pagel (2004) N2 diagnostic to these H II regions; there is a fairly large scatter inherent in the diagnostic. We plot six low- z GRB/SN hosts (red circles) to show the similarity in metallicity trends for luminous SNe and GRB hosts (Chornock et al. 2010; Levesque et al. 2010a).

For high-luminosity SNe which do not yet have direct host metallicity measurements, we plot arrows at the host absolute magnitudes or at the upper limit the host absolute

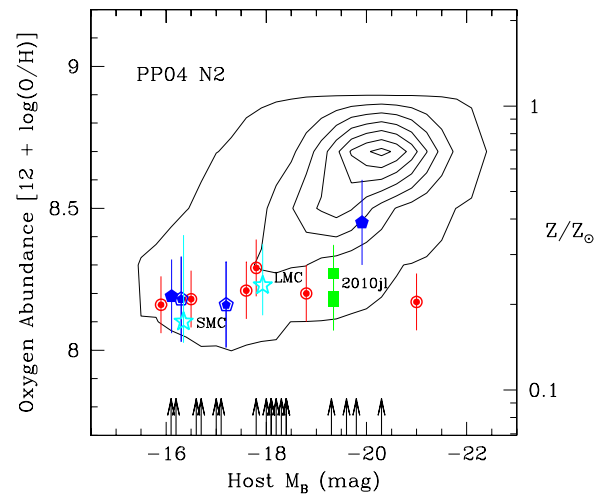


Figure 5. Host galaxy metallicities and absolute magnitudes are plotted for luminous SNe (blue pentagons) including SN 2010jl (green squares). The luminous supernovae without detected hydrogen (SN 2010gx and SN 2007bi) are indicated with double pentagons. The contours show the distribution of SDSS galactic metallicities from Tremonti et al. (2004). For comparison we plot the host galaxies of low-redshift long GRBs (red points) showing that both they and the luminous SNe hosts appear primarily in the low-metallicity tail of the galaxy distribution. We calculate abundances of the (Russell & Dopita 1990) sample of H II regions for the LMC and SMC calculated with the N2 diagnostic of Pettini & Pagel (2004) and plot ranges and medians with cyan stars. (We stress that the actual ranges in the LMC and SMC metallicities are likely lower than the ranges given by applying the Pettini & Pagel (2004) N2 diagnostic to these H II regions; there is a fairly large scatter inherent in the diagnostic.) Host galaxies of luminous SNe that have no measurements yet of host metallicity are indicated with arrows at their absolute B magnitude. The right vertical axis shows the corresponding scale of oxygen abundance in terms of the solar value from Delahaye & Pinsonneault (2006). All metallicity measurements have been converted to the scale of the N2 diagnostic of Pettini & Pagel (2004) using the conversions of Kewley & Ellison (2008).

(A color version of this figure is available in the online journal.)

magnitude (from left to right: SN 2005ap, SN 2006tf, SN 2008fz, SN 2005gj, PTF 10hgi, SN 2008es, PTF 10heh, PTF 09cnd, SCP06F6, PTF 10vqv, SN 2009jh, SN 1999as, PTF 09atu, and SN 2006gy). By comparing the distribution of these to the Tremonti et al. (2004) contours, it is clear that the host galaxies of these luminous SNe are in fainter galaxies. Neill et al. (2011) have also shown that the host galaxies of the most luminous SNe are the faintest, bluest galaxies. These hosts for which the metallicity have not yet been determined themselves provide support for the low-metallicity trend among luminous SNe hosts, because the faintest galaxies tend to be the most metal-poor (e.g., Tremonti et al. 2004).

These metallicity determinations were made with a number of different diagnostics, and so we have converted all to a single scale using the empirical conversions of Kewley & Ellison (2008). To emphasize that the low-metallicity trend is not an artifact of the particular common scale we choose, we plot the same thing on two different scales, that of the N2 diagnostic of Pettini & Pagel (2004) in Figure 5 and that of Denicoló et al. (2002) and Tremonti et al. (2004) in Figure 6. These were chosen to avoid a gap in the range where the Kewley & Ellison (2008) conversions from Tremonti et al. (2004) are valid. Slightly under 2% of the galaxies plotted have Tremonti et al. (2004) metallicities outside the 8.05–9.2 span where the Kewley & Ellison (2008) conversions are valid (mostly > 9.2), and these are excluded from the contour plot; the flat contour at the top of each plot is due to this exclusion. In Figure 6, we approximated the Kewley & Dopita (2002) metallicity of GRB020903 as

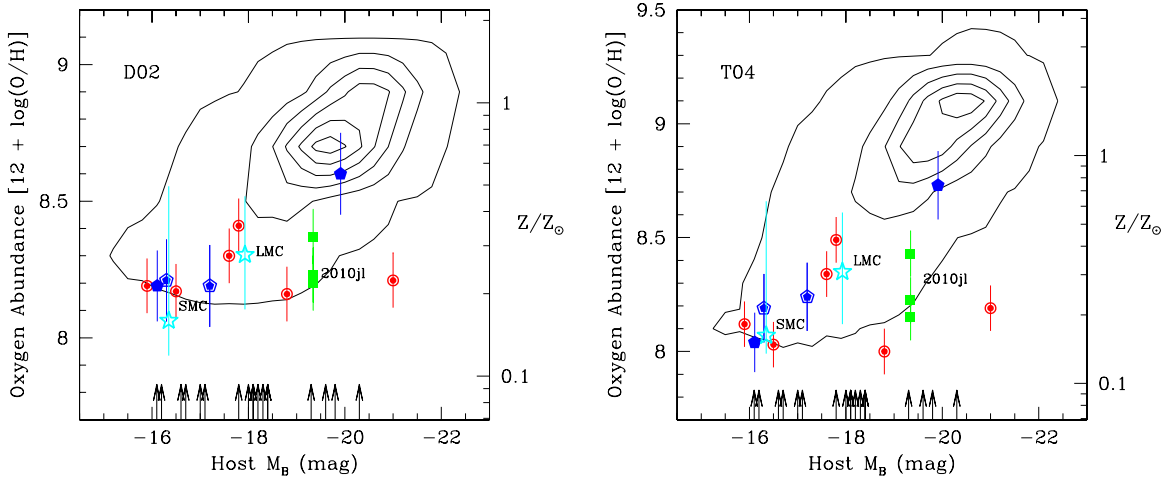


Figure 6. Same as Figure 5, except (left) with all metallicities on or converted to the scale of the Denicoló et al. (2002) strong-line diagnostic, or (right) with all metallicities on or converted to the scale of the Tremonti et al. (2004) diagnostic. We emphasize that the low-metallicity trend is not an artifact of which metallicity scale one prefers.

(A color version of this figure is available in the online journal.)

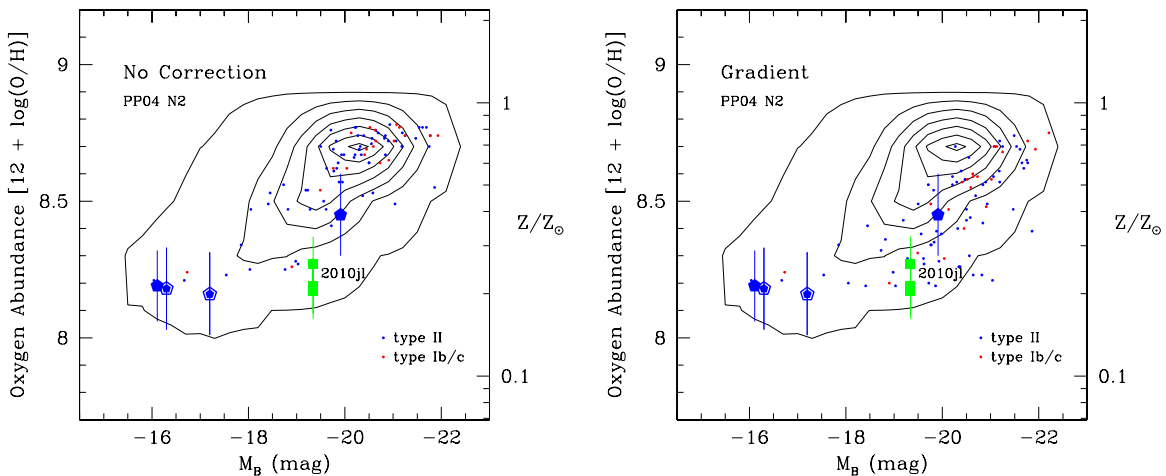


Figure 7. Type II and type Ib/c SNe that have hosts with SDSS spectra and metallicities (Tremonti et al. 2004) are plotted in the same way as Figure 5. On the left, the galactic metallicities have been approximately corrected for metallicity gradients to the position of the SN. On the right, no such correction has been made. As in previous figures, all metallicities have been corrected to the scale of the Pettini & Pagel (2004) N2 diagnostic using the conversions of Kewley & Ellison (2008). The hosts of the overluminous SNe from Figure 5 have been plotted here again for reference.

(A color version of this figure is available in the online journal.)

8.1 instead of 8.07 ± 0.1 in order for the Kewley & Ellison (2008) conversion to be valid, and averaged the converted metallicities from the N2 scale of Pettini & Pagel (2004) and Denicoló et al. (2002) for the LMC, the SMC, and the north and south galaxy regions of the host of SN 2010jl observed by OSMOS. On each of these three scales, the low-metallicity trend is clear.

Prieto et al. (2008) found that SN Ib/c occur more frequently in higher-metallicity galaxies compared to SN II and SN Ia. The highly luminous SNe we show in Figure 5 appear to show a larger bias toward low-metallicity hosts than normal SN Ib/c. For comparison, in Figure 7 we plot host metallicities for type II and type Ib/c SNe that have hosts that have SDSS spectra and are in the redshift range $0.04 > z > 0.01$. We caution that these SNe are from many different surveys, each of which has its own selection biases. On the left, the galactic metallicities are provided as observed, in the central three arcseconds of the galaxy. On the right, they have been approximately corrected to the position of the SN for the expected metallicity gradient often observed in similar galaxies.

We use an empirical formula for the metallicity gradient in dex kpc^{-1} as a function of absolute B magnitude of the host galaxy that is derived from the data published in Moustakas & Kennicutt (2006). We assume that dwarf galaxies with $M_B > -18$ mag are chemically homogeneous, and we assume no correction to the metallicity for SNe within the $1''.5$ radius of the SDSS fiber.

To roughly quantify the difference, we performed Kolmogorov–Smirnov tests and found that for the naive (and likely incorrect) assumption of uniform selection, the probability of the luminous SNe and the type II or type Ib/c SNe progenitor regions being drawn from the same distribution in metallicity ranges from 3.9×10^{-4} to 5.6×10^{-5} . Given the very different selection functions of these samples, though, this is in no way statistically rigorous and should merely be taken as thought provoking. Some related results have been recently shown to hold for homogeneous and untargeted samples; Arcavi et al. (2010) show that there is a significant excess of SNe IIB in dwarf hosts, and that while normal SNe Ic dominate in giant

galaxies, all type I core-collapse events in dwarf galaxies are type Ib or broad-lined type Ic.

4. DISCUSSION

The metallicities of the hosts of SN 2010jl and SN 2010gx support and strengthen the emerging trend that luminous SNe occur preferentially in metal-poor hosts. This result suggests that luminous SNe have low-metallicity progenitors. It is an interesting parallel to the similar trend observed for the hosts of long GRBs. The trend is not an artifact of which metallicity diagnostic is chosen for the host galaxies.

The relative iron abundance of these metal-poor hosts is expected to be even lower than suggested by the oxygen abundance that we use as a proxy for metallicity. At low metallicity, α -elements like oxygen are enhanced relative to iron, compared to the solar mixture. In the galactic disk and halo, at $[\text{Fe}/\text{H}] > -1$, $[\text{O}/\text{Fe}]$ is approximately inversely proportional to $[\text{Fe}/\text{H}]$, while below $[\text{Fe}/\text{H}] = -1$, the relationship flattens out at a constant (and lower) relative iron abundance (e.g., Tinsley 1979; McWilliam 1997; Johnson et al. 2007). The iron abundance is more fundamentally important for the late-stage evolution of massive stars because iron provides much of the opacity for radiation-driven stellar winds (e.g., Pauldrach et al. 1986; Vink & de Koter 2005). By using oxygen abundance as a metallicity tracer, we are in fact underestimating the magnitude of the effect of low metallicity on mass loss. If there is a threshold in iron abundance for certain types of luminous SNe, the observed effect in oxygen abundance will be less pronounced. The substantial preference we see for these SNe to occur in hosts with low nebular abundance of oxygen points to a more stringent constraint in iron abundance.

Nebular oxygen abundances determined by electron temperature methods appear to track the stellar abundances of massive young stars very closely, as Bresolin et al. (2009) demonstrate by comparing the gas-phase metallicity gradient from H II regions to the gradient in stellar abundances in NGC 300, so the gas-phase oxygen abundances we discuss should well characterize the stellar abundances of the massive young progenitors of these SNe.

A number of observational results for normal SN Ib/c and SN II support a change in their number ratios as a function of metallicity. In an early study, Prantzos & Boissier (2003) used the absolute magnitudes of SN host galaxies as a proxy for their average metallicities from the luminosity–metallicity relationship, and found that the number ratio of normal SN Ib/c to SN II increases with metallicity. Prieto et al. (2008) took advantage of the large sample of well-observed and typed SNe in the literature with star-forming host galaxies that have high S/N spectra obtained by the SDSS. They found strong evidence that normal SN Ib/c, dominated in rates by SN Ic, occur more frequently in higher-metallicity galaxies compared to SN II and SN Ia. Recently, Modjaz et al. (2010) found that the local metallicity of the hosts of SN Ic is on average higher than for hosts of SN Ib (but see Anderson et al. 2010). All these results are consistent with state-of-the-art stellar evolution models of massive stars with rotation, either single or in binaries (e.g., Eldridge et al. 2008; Georgy et al. 2009, 2011).

Studies of local and cosmological long-duration GRBs find that their host galaxies have low metallicity compared to the general population of star-forming galaxies and other CCSNe. These results help put constraints on progenitor models and the physics of production of the GRB jet, and they have fundamental implications for the use of GRBs as star formation

tracers at high redshift (e.g., Kistler et al. 2009). Fruchter et al. (2006) initially pointed out that the host environments of cosmological GRBs were different from CCSNe, with GRBs being hosted by strongly star-forming dwarf galaxies (see also Le Floc'h et al. 2003). Stanek et al. (2006) compared direct host metallicity measurements of five local GRBs with those of star-forming galaxies in SDSS, and found that long GRBs prefer low-metallicity environments. This result has recently been confirmed using a larger sample of events (Levesque et al. 2010b). Modjaz et al. (2008) used direct host galaxy metallicity estimates to study nearby broad-lined SN Ic. They find that the metallicities of hosts of SN Ic without GRB are higher than the metallicities of hosts of SN Ic associated with GRBs.

4.1. Luminous Supernovae

One of the most surprising results of the new transient surveys that are monitoring many square degrees of the sky every few nights has been the discovery of very luminous SNe in the nearby universe that are ~ 10 times more luminous than normal CCSNe and can release $\sim 10^{51}$ erg in UV–optical light.

The first events of this kind were SN 2005ap (Quimby et al. 2007) and SN 2006gy (Smith et al. 2007), discovered by TSS. Their light curves, spectral properties, and environments are remarkably different, although they both share extreme energetics compared to normal CCSNe. SN 2005ap was discovered in a low-luminosity galaxy at $z = 0.28$. It showed a relatively fast evolution in its light curve, but with an extreme peak absolute magnitude of -23 mag never before seen in an SN. The spectra had very broad features that were mainly associated with CNO events. The absence of hydrogen in the spectrum, the features at high velocity, and the extreme energetics led Quimby et al. (2007) to propose that SN 2005ap could be associated with long GRBs, which connected this event with a high-mass progenitor star.

SN 2006gy was discovered close to the center of a nearby ($z = 0.02$) S0 galaxy with recent star formation. Its spectrum and light curve were similar to type II_n SNe, but they were much more extreme, with a peak absolute magnitude of -22 and clear signs of interaction between the SN ejecta and a massive, hydrogen-rich circumstellar shell. This led Smith et al. (2007) to propose that the progenitor of SN 2006gy had been a very massive star (initial mass $\gtrsim 100 M_{\odot}$) similar to the well-studied galactic LBV η -Carinae. The explosion mechanism of SN 2006gy might be explained by the pulsational pair-instability model (Woosley et al. 2007).

van Marle et al. (2010) explore possible models for luminous type II_n SNe and find within the parameter space that they explore that sustained high luminosity requires massive circumstellar shells. Metzger (2010) consider interaction with a relic protostellar disk, finding that when the disk is massive and compact and the cooling time is long compared to the expansion timescale, more of the energy is radiated in the optical, which they suggest is a possible explanation of luminous type II_n events. Murase et al. (2010) explore potential consequences of such interactions with circumstellar shells for the production of gamma rays and neutrinos.

If LBV-like stars are the progenitors of these extremely luminous SNe, that does not constrain them to live in high-metallicity environments; LBVs have been identified in galaxies with $12 + \log(\text{O}/\text{H}) \lesssim 8.0$ (Izotov & Thuan 2009; Herrero et al. 2010). The progenitor of the luminous type II_n SN 2010jl is constrained by Smith et al. (2010b) to be a massive LBV, a less

Table 2
List of Luminous CCSNe Collected from the Literature

SN Name	R.A. (J2000.0)	Decl. (J2000.0)	SN Spectral Type	Redshift	$M_B(\text{host})$ (mag)	Host Metallicity? (12+log[O/H], PP04N2)
SN 1995av	02:01:36.7	03:38:55	IIn	0.3	...	No
SN 1997cy	04:32:54.8	-61:42:57	IIn	0.063	-17.8	No
SN 1999as	09:16:30.8	+13:39:02	Ic	0.13	-18.4	No
SN 1999bd	09:30:29.2	+16:26:08	IIn	0.151	-18.4	No
SN 2000ei	04:17:07.2	+05:45:53	IIn	0.600	> -19.3	No
SN 2003ma	05:31:01.9	-70:04:16	IIn	0.29	-19.9	8.45
SN 2005ap	13:01:14.8	+27:43:31	Ic?	0.28	-16.1	No
SN 2005gj	03:01:12.0	+00:33:14	Ia/IIn	0.06	-16.7	No
SCP06F6	14:32:27.4	+33:32:25	Ic?	1.19	> -18.1	No
SN 2006gy	03:17:27.0	+41:24:20	IIn	0.02	-20.3	No
SN 2006tf	11:56:49.1	+54:27:26	IIn	0.07	-16.2	No
SN 2007bi	13:19:20.2	+08:55:44	Ic	0.13	-16.3	8.18
SN 2007va	14:26:23.2	+35:35:29	IIn?	0.19	-16.2	8.19
SN 2008am	12:28:36.2	+15:34:49	IIn	0.234	-19.6	No
SN 2008es	12:46:15.8	+11:25:56	IIL	0.21	> -17.1	No
SN 2008fz	23:16:16.6	+11:42:48	IIn	0.13	> -16.6	No
PTF 09atu	16:30:24.6	+23:38:25	Ic?	0.50	> -19.8	No
PTF 09cnd	16:12:08.9	+51:29:16	Ic?	0.26	> -18.1	No
SN 2009jh	14:49:10.1	+29:25:11	Ic?	0.35	> -18.3	No
SN 2010gx	11:25:46.7	-08:49:41	Ic?	0.23	-17.2	8.16
PTF 10heh	12:48:52.0	+13:26:24.5	IIn	0.34	-18.0	No
PTF 10hgi	16:37:47.0	+06:12:32.3	Ic?	0.10	> -17.0	No
PTF 10vqv	03:03:06.8	-01:32:34.9	Ic?	0.45	-18.2	No
SN 2010jl	09:42:53.3	+09:29:41.8	IIn	0.01	-19.3	8.19

massive object temporarily experiencing an LBV-like eruption in a precursor explosion, or a member of a compact, massive cluster with turnoff mass $\gtrsim 30 M_{\odot}$. The progenitors of two less luminous type IIn events have been identified. One of these, SN 2005gl, occurred in a region with gas-phase metallicity of $12 + \log(\text{O}/\text{H}) = 9.1 \pm 0.3$, and its progenitor was identified as an LBV with $M_V = -10.3$ (Gal-Yam & Leonard 2009). The other, SN 1961V, a low-metallicity, normal-luminosity type IIn (Kochanek et al. 2010; Smith et al. 2010a), had a progenitor with $M_{\text{ZAMS}} > 80 M_{\odot}$, which must have been greater than $\sim 30 M_{\odot}$ at the time of explosion to retain any hydrogen (Kochanek et al. 2010).

Since the discovery of SN 2005ap and SN 2006gy, there have been several very energetic SNe (peak $M_R < -20$) discovered by different surveys out to redshift $z \approx 1$. We present a list in Table 2; we include whether each event is classified as type I (without hydrogen) or type II (with hydrogen). Many host absolute B magnitudes are converted and errors might be ~ 0.2 mag or larger. The new discoveries include objects with a variety of properties. Some events are similar to SN 2005ap, including SCP06F6, PTF 09cnd, PTF 09atu, and SN 2009jh (Quimby et al. 2009), SN 2010gx (Mahabal et al. 2010; Quimby et al. 2010a; Mahabal & Drake 2010; Pastorello et al. 2010), PTF 10hgi (Quimby et al. 2010c), and PTF 10vqv (Quimby et al. 2010d), and to SN 2006gy, including SN 2003ma (Rest et al. 2009), SN 2005gj (Aldering et al. 2006; Prieto et al. 2007), SN 2006tf (Smith et al. 2008), SN 2008es (Miller et al. 2009; Gezari et al. 2009), SN 2008fz (Drake et al. 2010), and PTF 10heh (Quimby et al. 2010b). Others are more similar to broad-lined SN Ic in spectroscopic properties, but with extreme luminosity, such as SN 1999as and SN 2007bi (Gal-Yam et al. 2009). We also include a unique event, SN 2007va, that was completely enshrouded in its own circumstellar dust and only observable at mid-infrared wavelengths; its infrared luminosity indicated high reprocessed optical luminosity (Kozłowski et al.

2010). The most recent example (and nearest, at $z = 0.011$) is the type IIn SN 2010jl, the main subject of this paper. The variety of observed properties in these luminous CCSNe likely represents different explosion mechanisms (e.g., normal collapse of the core versus pair instability versus pulsational pair instability), different mechanisms that power the energetics of the light curves (e.g., circumstellar interaction versus radioactive decay versus magnetar spin down), and different progenitor mass-loss histories and masses (e.g., LBV versus Wolf-Rayet stars versus red supergiants).

4.2. Metallicity Diagnostics

The forbidden and recombination lines in the optical spectra of star-forming galaxies provide the observables needed to estimate chemical abundances, star formation rates, and other physical properties of the H II regions, such as electron temperature and density. These emission lines are produced by collisional excitation and recombination processes in gaseous nebulae where massive ($\gtrsim 20 M_{\odot}$) stars form, thanks to the interactions of the ionizing UV photons provided by the stars and the surrounding gas (e.g., Osterbrock & Ferland 2006).

There is a vast literature on a number of techniques that have been developed over the last three decades to estimate the oxygen abundances and physical conditions of H II regions in star-forming galaxies (e.g., Kewley & Ellison 2008, and references therein). The methods can be divided into four different categories: direct (uses an estimate of the electron temperature measured from the faint [O III] λ 4363 auroral line), empirical (e.g., Pettini & Pagel 2004), theoretical (e.g., Kobulnicky & Kewley 2004), and a combination of empirical and theoretical (e.g., Denicoló et al. 2002). All these methods are based on high S/N measurements of the line ratios of different combinations of emission lines from ions present in the optical region of the spectrum ($\simeq 3700\text{--}6700 \text{ \AA}$): [O II], [O III], [N II], [S II], H α , and H β .

Each method has relative advantages and shortcomings that have been investigated in a number of studies in the literature (e.g., Yin et al. 2007; Moustakas et al. 2010), and there are known discrepancies of as much as ~ 0.6 dex between different estimates of the oxygen abundances. For example, the estimated oxygen abundance of the host galaxy of the luminous SN 2007va (Kozłowski et al. 2010) obtained from the direct electron temperature method is 0.3 dex lower than the value obtained from the theoretical calibration of $R_{23} = ([\text{O II}]\lambda 3727 + [\text{O III}]\lambda\lambda 4959, 5007)/\text{H}\beta$ (Kobulnicky & Kewley 2004). Bresolin et al. (2009) demonstrate the offsets between the various techniques for their determination of the metallicity gradient in NGC 300. The abundances estimated with one diagnostic, the N2 diagnostic of Pettini & Pagel (2004), essentially track the stellar and (T_e) nebular abundances they measure, albeit with rather more scatter. Because the effective zero points and scales vary somewhat, regardless of which method is used, it is important to use (or convert to) just one.

With the S/N and wavelength coverage of our observations, we content ourselves in this paper with the empirical O3N2 and N2 diagnostics of Pettini & Pagel (2004) and the theoretical and empirical N2 diagnostic of Denicoló et al. (2002). We use the empirical conversions of Kewley & Ellison (2008) to convert metallicities determined on other scales to these for the purpose of direct comparison.

5. CONCLUSIONS

Recent observations of the environments of SNe and GRBs show that metallicity is a key parameter in the lives and deaths of massive stars. Our finding that the hosts of luminous SNe lie in the low-metallicity extremes of the distribution of star-forming galaxies supports this emerging picture. Verifying and constraining this emerging relationship with metallicity may be an important probe of the mechanisms of the most luminous SNe, and this trend may be an important factor in various aspects of the evolution of the metal-poor early universe.

We thank Andrew Drake, Avishay Gal-Yam, Jennifer Johnson, Rubab Khan, Chris Kochanek, Paul Martini, Brian Metzger, Nidia Morrell, Rupak Roy, Josh Simon, Firoza Sutaria, and the anonymous referee for discussion, comments, and assistance. J.L.P. acknowledges support from NASA through Hubble Fellowship grant HF-51261.01-A awarded by the STScI, which is operated by AURA, Inc. for NASA, under contract NAS 5-26555. R.S. is supported by the David G. Price Fellowship in Astronomical Instrumentation. G.P. is supported by the Polish MNiSW grant N203 007 31/1328. OSMOS has been generously funded by the National Science Foundation (AST-0705170) and the Center for Cosmology and AstroParticle Physics at The Ohio State University. Funding for the SDSS and SDSS-II has been provided by the Alfred P. Sloan Foundation, the Participating Institutions, the National Science Foundation, the U.S. Department of Energy, the National Aeronautics and Space Administration, the Japanese Monbukagakusho, the Max Planck Society, and the Higher Education Funding Council for England. The SDSS Web site is <http://www.sdss.org/>. The SDSS is managed by the Astrophysical Research Consortium for the Participating Institutions. The Participating Institutions are the American Museum of Natural History, Astrophysical Institute Potsdam, University of Basel, University of Cambridge, Case Western Reserve University, University of Chicago, Drexel University, Fermilab, the Institute for Advanced Study, the Japan Participation Group, Johns Hopkins University, the Joint Institute for

Nuclear Astrophysics, the Kavli Institute for Particle Astrophysics and Cosmology, the Korean Scientist Group, the Chinese Academy of Sciences (LAMOST), Los Alamos National Laboratory, the Max-Planck-Institute for Astronomy (MPIA), the Max-Planck-Institute for Astrophysics (MPA), New Mexico State University, Ohio State University, University of Pittsburgh, University of Portsmouth, Princeton University, the United States Naval Observatory, and the University of Washington. This research has made use of the NASA/IPAC Extragalactic Database (NED) which is operated by the Jet Propulsion Laboratory, California Institute of Technology, under contract with the National Aeronautics and Space Administration.

Facilities: Hiltner (OSMOS), Sloan, Du Pont (WFCCD), Swope

REFERENCES

- Abazajian, K. N., et al. 2009, *ApJS*, 182, 543
 Aldering, G., et al. 2006, *ApJ*, 650, 510
 Anderson, J. P., Covarrubias, R. A., James, P. A., Hamuy, M., & Haberman, S. M. 2010, *MNRAS*, 407, 2660
 Arcavi, I., et al. 2010, *ApJ*, 721, 777
 Benetti, S., Bufano, F., Vinko, J., Marion, G. H., Pritchard, T., Wheeler, J. C., Chatzopoulos, E., & Shetrone, M. 2010, *CBET*, 2536, 1
 Bresolin, F., Gieren, W., Kudritzki, R., Pietrzyński, G., Urbaneja, M. A., & Carraro, G. 2009, *ApJ*, 700, 309
 Brinchmann, J., Kunth, D., & Durret, F. 2008, *A&A*, 485, 657
 Chornock, R., et al. 2010, arXiv:1004.2262
 Delahaye, F., & Pinsonneault, M. H. 2006, *ApJ*, 649, 529
 Denicoló, G., Terlevich, R., & Terlevich, E. 2002, *MNRAS*, 330, 69
 Drake, A. J., et al. 2009, *ApJ*, 696, 870
 Drake, A. J., et al. 2010, *ApJ*, 718, L127
 Eldridge, J. J., Izzard, R. G., & Tout, C. A. 2008, *MNRAS*, 384, 1109
 Fassia, A., et al. 2000, *MNRAS*, 318, 1093
 Fruchter, A. S., et al. 2006, *Nature*, 441, 463
 Gal-Yam, A., & Leonard, D. C. 2009, *Nature*, 458, 865
 Gal-Yam, A., et al. 2009, *Nature*, 462, 624
 Garnett, D. R., Kennicutt, R. C., Jr., Chu, Y., & Skillman, E. D. 1991, *ApJ*, 373, 458
 Georgy, C., Meynet, G., & Maeder, A. 2011, *A&A*, 527, 52
 Georgy, C., Meynet, G., Walder, R., Folini, D., & Maeder, A. 2009, *A&A*, 502, 611
 Germany, L. M., Reiss, D. J., Sadler, E. M., Schmidt, B. P., & Stubbs, C. W. 2000, *ApJ*, 533, 320
 Gezari, S., et al. 2009, *ApJ*, 690, 1313
 Hamuy, M., et al. 2006, *PASP*, 118, 2
 Herrero, A., Garcia, M., Uytterhoeven, K., Najarro, F., Lennon, D. J., Vink, J. S., & Castro, N. 2010, *A&A*, 513, A70
 Hög, E., et al. 2000, *A&A*, 355, L27
 Iztov, Y. I., & Thuan, T. X. 2009, *ApJ*, 690, 1797
 Johnson, J. A., Gal-Yam, A., Leonard, D. C., Simon, J. D., Udalski, A., & Gould, A. 2007, *ApJ*, 655, L33
 Karachentsev, I. D. 2005, *AJ*, 129, 178
 Kewley, L. J., & Dopita, M. A. 2002, *ApJS*, 142, 35
 Kewley, L. J., & Ellison, S. L. 2008, *ApJ*, 681, 1183
 Kiewe, M., et al. 2010, arXiv:1010.2689
 Kistler, M. D., Yüksel, H., Beacom, J. F., Hopkins, A. M., & Wyithe, J. S. B. 2009, *ApJ*, 705, L104
 Kobulnicky, H. A., & Kewley, L. J. 2004, *ApJ*, 617, 240
 Kochanek, C. S., Szczygiel, D. M., & Stanek, K. Z. 2010, arXiv:1010.3704
 Kozłowski, S., et al. 2010, *ApJ*, 722, 1624
 Landolt, A. U. 1983, *AJ*, 88, 439
 Le Floch, E., et al. 2003, *A&A*, 400, 499
 Levesque, E. M., Berger, E., Kewley, L. J., & Bagley, M. M. 2010a, *AJ*, 139, 694
 Levesque, E. M., Kewley, L. J., Berger, E., & Jabran Zahid, H. 2010b, *AJ*, 140, 1557
 Li, W., et al. 2010, arXiv:1006.4612
 Mahabal, A. A., & Drake, A. J. 2010, *ATel*, 2508, 1
 Mahabal, A. A., et al. 2010, *ATel*, 2490, 1
 Martini, P., et al. 2011, *PASP*, in press
 McWilliam, A. 1997, *ARA&A*, 35, 503
 Metzger, B. D. 2010, *MNRAS*, 409, 284
 Miller, A. A., et al. 2009, *ApJ*, 690, 1303

- Modjaz, M., Bloom, J. S., Filippenko, A. V., Kewley, L., Perley, D., & Silverman, J. M. 2010, arXiv:1007.0661
- Modjaz, M., et al. 2008, *AJ*, **135**, 1136
- Moustakas, J., & Kennicutt, R. C., Jr. 2006, *ApJ*, **651**, 155
- Moustakas, J., Kennicutt, R. C., Jr., Tremonti, C. A., Dale, D. A., Smith, J., & Calzetti, D. 2010, *ApJS*, **190**, 233
- Murase, K., Thompson, T. A., Lacki, B. C., & Beacom, J. F. 2010, arXiv:1012.2834
- Neill, J. D., et al. 2011, *ApJ*, **727**, 15
- Newton, J., & Puckett, T. 2010, CBET, **2532**, 1
- Oke, J. B. 1990, *AJ*, **99**, 1621
- Osterbrock, D. E., & Ferland, G. J. (ed.) 2006, *Astrophysics of Gaseous Nebulae and Active Galactic Nuclei* (Sausalito, CA: Univ. Science Books)
- Pastorello, A., et al. 2010, *ApJ*, **724**, L16
- Patat, F., Taubenberger, S., Benetti, S., Pastorello, A., & Harutyunyan, A. 2010, arXiv:1011.5926
- Pauldrach, A., Puls, J., & Kudritzki, R. P. 1986, *A&A*, **164**, 86
- Peeples, M. S., Pogge, R. W., & Stanek, K. Z. 2009, *ApJ*, **695**, 259
- Pettini, M., & Pagel, B. E. J. 2004, *MNRAS*, **348**, L59
- Pigulski, A., Pojmański, G., Pilecki, B., & Szczygieł, D. M. 2009, *Acta Astron.*, **59**, 33
- Pilyugin, L. S., & Thuan, T. X. 2007, *ApJ*, **669**, 299
- Pojmanski, G. 1998, *Acta Astron.*, **48**, 35
- Pojmanski, G. 2002, *Acta Astron.*, **52**, 397
- Prantzos, N., & Boissier, S. 2003, *A&A*, **406**, 259
- Prieto, J. L., & Stanek, K. Z. 2010, ATel, **3010**, 1
- Prieto, J. L., Stanek, K. Z., & Beacom, J. F. 2008, *ApJ*, **673**, 999
- Prieto, J. L., et al. 2007, arXiv:0706.4088
- Quimby, R. M. 2006, PhD thesis, Univ. Texas at Austin
- Quimby, R. M., Aldering, G., Wheeler, J. C., Höflich, P., Akerlof, C. W., & Rykoff, E. S. 2007, *ApJ*, **668**, L99
- Quimby, R. M., Kulkarni, S. R., Ofek, E., Kasliwal, M. M., Levitan, D., Gal-Yam, A., & Cenko, S. B. 2010a, ATel, **2492**, 1
- Quimby, R. M., et al. 2009, arXiv:0910.0059
- Quimby, R. M., et al. 2010b, ATel, **2634**, 1
- Quimby, R. M., et al. 2010c, ATel, **2740**, 1
- Quimby, R. M., et al. 2010d, ATel, **2979**, 1
- Rau, A., et al. 2009, *PASP*, **121**, 1334
- Rest, A., et al. 2009, arXiv:0911.2002
- Rigon, L., et al. 2003, *MNRAS*, **340**, 191
- Russell, S. C., & Dopita, M. A. 1990, *ApJS*, **74**, 93
- Smith, N., Chornock, R., Li, W., Ganeshalingam, M., Silverman, J. M., Foley, R. J., Filippenko, A. V., & Barth, A. J. 2008, *ApJ*, **686**, 467
- Smith, N., Li, W., Silverman, J. M., Ganeshalingam, M., & Filippenko, A. V. 2010a, arXiv:1010.3718
- Smith, N., et al. 2007, *ApJ*, **666**, 1116
- Smith, N., et al. 2010b, arXiv:1011.4150
- Stanek, K. Z., et al. 2003, *ApJ*, **591**, L17
- Stanek, K. Z., et al. 2006, *Acta Astron.*, **56**, 333
- Stoll, R., et al. 2010, *Proc. SPIE*, **7735**, 154
- Tinsley, B. M. 1979, *ApJ*, **229**, 1046
- Tremonti, C. A., et al. 2004, *ApJ*, **613**, 898
- van Dokkum, P. G. 2001, *PASP*, **113**, 1420
- van Marle, A. J., Smith, N., Owocki, S. P., & van Veelen, B. 2010, *MNRAS*, **407**, 2305
- Vink, J. S., & de Koter, A. 2005, *A&A*, **442**, 587
- Woosley, S. E., Blinnikov, S., & Heger, A. 2007, *Nature*, **450**, 390
- Yamanaka, M., Okushima, T., Arai, A., Sasada, M., & Sato, H. 2010, CBET, **2539**, 1
- Yin, S. Y., Liang, Y. C., Hammer, F., Brinchmann, J., Zhang, B., Deng, L. C., & Flores, H. 2007, *A&A*, **462**, 535